Quaternary Science Reviews 193 (2018) 54–67

Contents lists available at ScienceDirect

Quaternary Science Reviews

journal homepage: www.elsevier.com/locate/quascirev

Decoupled early Holocene summer temperature and monsoon precipitation in southwest China

Duo Wu [a], Xuemei Chen [b], Feiya Lv [a], Mark Brenner [c], Jason Curtis [c], Aifeng Zhou [a], Jianhui Chen [a], Mark Abbott [d], Junqing Yu [e], Fahu Chen [a, f, *]

[a] College of Earth and Environmental Sciences, MOE Key Laboratory of Western China's Environmental System, Lanzhou University, Lanzhou, 730000, China
[b] State Key Laboratory of Frozen Soils Engineering, Northwest Institute of Eco-Environment and Resources, Chinese Academy of Science, Lanzhou, 730000, China
[c] Department of Geological Sciences and Land Use and Environmental Change Institute, University of Florida, Gainesville, 32611, USA
[d] Department of Geology and Environmental Science, University of Pittsburgh, Pittsburgh, 15260, USA
[e] Qinghai Institute of Salt Lake Studies, Chinese Academy of Sciences, Xining, 810008, China
[f] Institute of Tibetan Plateau Research, Chinese Academy of Sciences, Beijing, 100101, China

ARTICLE INFO

Article history:
Received 25 March 2018
Received in revised form
28 May 2018
Accepted 29 May 2018

Keywords:
Indian summer monsoon
Mean July temperature
Xingyun Lake
Early Holocene
Decoupled variation

ABSTRACT

Proxy-based reconstructions of Holocene temperature show that both the timing and magnitude of the thermal maximum varied substantially across different regions. Given the 'Holocene temperature conundrum', it is becoming increasingly important to reconstruct seasonal temperature variations. As a major component of the global monsoon system, the Indian summer monsoon (ISM) transports moisture and heat from the tropical oceans to higher latitudes and thus it has substantial socioeconomic implications for its regions of influences. We developed a well-dated, pollen-based summer temperature record (mean July; MJT) for the last 14,000 years from Xingyun Lake in southwest China, where the climate is dominated by the ISM. MJT decreased during the Younger Dryas, increased slowly to high values during 8000–5500 yr BP, and decreased thereafter. The MJT record differs from that inferred using carbonate oxygen isotopes ($\delta^{18}O$) from the same sediment core. The latter record reflects variations in monsoon precipitation, with highest precipitation during the early Holocene (11,000–6500 yr BP). We propose that summer temperature and precipitation in southwest China were decoupled during the early Holocene. Both MJT and monsoon precipitation decreased after the middle Holocene, tracking the trend in boreal summer insolation. We suggest that greater cloud cover, associated with high precipitation and generated by a strong summer monsoon, may have depressed early Holocene temperatures that would otherwise be driven by greater summer insolation. Melting ice sheets in high-latitude regions and high concentrations of atmospheric aerosols during the early Holocene may also have contributed, in part, to the relatively cool summer temperatures.

1. Introduction

Using 73 globally distributed temperature records, Marcott et al. (2013) found that global annual temperature shows an early Holocene maximum, followed by a cooling trend through the middle to late Holocene which ended in the preindustrial era. This finding, however, disagrees with simulated global temperature variations that show a warming trend during the Holocene, mainly attributed to rising atmospheric greenhouse gas concentrations and retreating ice sheets (Liu et al., 2014). Liu et al. (2014) suggested that the cooling trend in the global stack is driven mainly by a bias towards summer temperature in the Northern Hemisphere, because temperature reconstructions are dominated by several alkenone-based sea-surface temperature records. These conflicting results, namely the so-called 'Holocene temperature conundrum', highlight the need to reassess the sensitivity of current climate models, and to pay more attention to possible seasonality effects in proxy reconstructions (Liu et al., 2014). Modeled simulations of Holocene

* Corresponding author. College of Earth and Environmental Sciences, MOE Key Laboratory of Western China's Environmental System, Lanzhou University, Lanzhou, 730000, China.
E-mail address: fhchen@lzu.edu.cn (F. Chen).

https://doi.org/10.1016/j.quascirev.2018.05.038
0277-3791/

summer temperatures show that summers were cooler over regions directly influenced by the Laurentide ice sheet during the early Holocene, whereas for areas elsewhere in the Northern Hemisphere, summer temperatures were dominated by orbital insolation (Renssen et al., 2009). Proxy-based reconstructions of Holocene temperature, however, have shown that both the timing and magnitude of the thermal maximum differed substantially among regions (Shi et al., 1993; Kaufman et al., 2004; Renssen et al., 2009; Zhang et al., 2017a, 2017b). The lack of summer temperature reconstructions from low-latitude land regions makes it difficult to establish temporal patterns of Holocene summer temperature variations across the broader landscape and to determine the underlying forcing mechanisms of temperature change.

The Indian summer monsoon (ISM) is a major component of the global monsoon system and it is initiated by differential sensible heating of continental and oceanic regions (Webster et al., 1998). The ISM plays a crucial role in transporting moisture and heat from the tropical ocean to higher latitudes (Fleitmann et al., 2003; An et al., 2011; Govil and Naidu, 2011). Changes in the ISM have substantial socioeconomic implications for regions under its influence, through changes in water availability. Currently, ISM variability, especially extreme precipitation conditions, can cause severe droughts or floods which affect large numbers of people (Webster et al., 1998). In response to recent global warming, precipitation in the ISM region has decreased substantially during the past half-century (Sinha et al., 2015) which potentially poses severe threats to terrestrial ecosystems. In addition, it was suggested that an increase in anthropogenic aerosols has caused a decrease in monsoonal precipitation in Asia during recent decades (Menon et al., 2002; Yu et al., 2016). Given the increase in human activities since the late 20th century, it is possible that the decoupling of temperature and ISM precipitation during the past half century is not linked to natural variability. On long timescales, it was found that precipitation in East Asia lagged the last deglacial warming by several thousand years (Peterse et al., 2011, 2014), and the timing of the Holocene ISM onset appears different with the beginning of warming (e.g., He et al., 2017). During the Holocene, climate boundary conditions were similar to those of today. Therefore we sought to investigate the natural variability of precipitation and temperature during the Holocene in the ISM domains, and to explore their underlying forcing mechanisms, to improve our ability to predict regional and global climate changes.

Yunnan Province, in southwest China, is within the area of ISM influence. Many tectonic (fault) lakes are distributed across the Yunnan Plateau. Although a substantial amount of paleoenvironmental research has been conducted on these lakes, including vegetation and climate reconstructions (Sun et al., 1986; Hodell et al., 1999; Shen et al., 2006; An et al., 2011; Cook et al., 2013; Chen et al., 2014a; Xiao et al., 2014; Zhang et al., 2017a), the regional patterns of Holocene climate and vegetation changes in the region are still poorly understood. For example, some studies detected an early Holocene climatic optimum (Cook et al., 2013; Chen et al., 2014a), whereas others suggest a middle or even late Holocene climatic optimum (Xiao et al., 2014). These differences limit our understanding of the evolution of the ISM during the Holocene. In addition, the lack of unambiguous precipitation and temperature records with robust chronologies from the same site also limits our ability to address the questions of whether precipitation and temperature respond directly, on orbital time scales, to Northern Hemisphere summer insolation forcing, without a phase lag, or whether the climate response is delayed by internal feedback mechanisms (Overpeck et al., 1996; Kutzbach et al., 2008; Clemens et al., 2010; An et al., 2011).

We have conducted detailed investigations of past climate using sediments from Xingyun Lake in Yunnan Province, southwest China (Chen et al., 2014a, 2014b; Hillman et al., 2014, 2017; Wu et al., 2015a, 2015b; Zhou et al., 2015). Because of possible hiatuses in our previously studied sediment cores (e.g., Chen et al., 2014a) we were unable to obtain continuous records that span the entire Holocene. In the present study, we compared records from a suite of cores, collected from different parts of the lake, to address the possible occurrence of a sedimentary hiatus in Xingyun Lake during the transition from the late glacial to the early Holocene. This enabled us to develop a composite record with robust age control, from multiple cores; then we used an analysis of fossil pollen assemblages to reconstruct past mean July temperature (MJT). Subsequently, we compared the temperature record with monsoonal precipitation records that were inferred from lacustrine carbonate oxygen isotope ($\delta^{18}O$) records to study their phase relationship and possible underlying forcing mechanisms.

2. Geographic setting

Xingyun Lake (24°17′20″N-24°23′05″N, 102°45′18″E–102°48′30″E) is a hydrologically closed, shallow ($z_{max} = 11$ m), eutrophic lake in central Yunnan Province, southwest China (Fig. 1A; Zhang et al., 2010). The lake surface lies at 1722 m above mean sea level (a.m.s.l.). The surface area is 34.7 km^2 and the catchment area is 386 km^2. Drainage into the basin is primarily via rainfall and runoff, including inflow from more than 14 rivers (Zhao and Zhao, 1988). The lake drained northwards via a narrow channel of the Gehe River into Fuxian Lake, and eventually into the Nanpan River system. Today, several dams on the Gehe River regulate the water flow. Xingyun Lake is a freshwater lake with conductivity of 344 μS/cm and the pH ranges from 8.4 to 8.7 (Song et al., 1994).

The lake lies within the ISM region (Fig. 1B), which has a monsoon climate characterized by warm, wet summers and cold, dry winters. Mean annual precipitation is ~1000 mm, with almost 80% falling from May to September, determined by instrumental measurements at the Kunming station, ~80 km north of Xingyun Lake, during the interval 1986–2003 (Fig. 1C). The climate of the region is relatively cool from October to April (mean 9–17 °C), and warm from May to September (mean 18–20 °C). Monsoon circulation strongly affects the isotopic composition of precipitation in Kunming and other areas dominated by the ISM, with lower $\delta^{18}O$ values during summer (Wei and Lin, 1994; Li et al., 2015b, 2016). The annual weighted mean $\delta^{18}O$ of modern rainfall at Kunming was −9.86‰ VSMOW and the $\delta^{18}O$ value of a water sample taken from Xingyun Lake in 2009 was −4.3‰ VSMOW, suggesting substantial evaporative water loss from the lake (Hillman et al., 2014).

The natural vegetation in the Xingyun Lake catchment is semi-humid, evergreen, broadleaved forest and pine forest, belonging to the subtropical evergreen broadleaved forest zone of the Yunnan Plateau (Editorial Board of Yunnan Vegetation in China, 1987). Because of human disturbance, however, most of the modern vegetation in the catchment consists mainly of cultivated plants and pine forest, with remnant broadleaved forest or shrubs, predominantly *Cyclobalanopsis delavayi, Castanopsis delavayi, Lithocarpus dealbatus, Quercus variabilis, Quercus senescens, Alnus nepalensis and Rhododendron* spp. (Editorial Board of Yunnan Vegetation in China, 1987; Chen et al., 2014b). The catchment geology includes dolomite, sandstone and sandy shale (Song et al., 1994), and *terra rossa* (red soil) is widely distributed in the catchment. Currently, the lake catchment contains large areas of flat land used for rice cultivation. The basin has experienced dramatic increases in soil erosion since about 500 CE, caused by increased deforestation and agricultural activity (Hillman et al., 2014; Wu et al., 2015a).

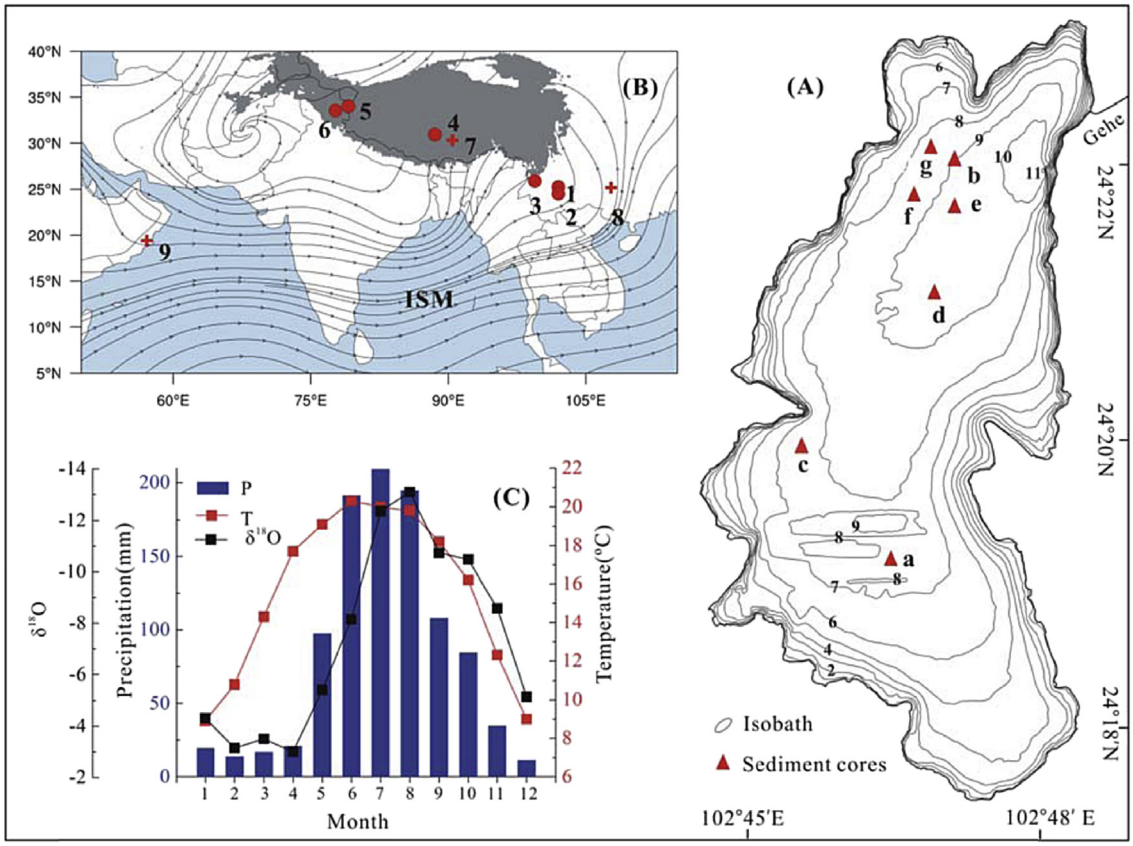

Fig. 1. Hydrological and climate information for the study area. (A) Bathymetry of Xingyun Lake and sediment core locations: a - XH-14-X-94 (Hodell et al., 1999); b - XYA09 (Hillman et al., 2014); c - core published in Zhang et al. (2014); d - XY08A (Chen et al., 2014a); e – XY08C, (Yu JQ, unpublished); f - XYB08 (Hillman et al., 2017); g - XH-3-IV-89 (Whitmore et al., 1994). (B) Main study sites in the Indian Summer Monsoon (ISM)-dominated region: 1 - Xingyun Lake (this study); 2 - Qilu Lake; 3 - Tiancai Lake; 4 - Selin Co; 5 - Bangong Co; 6 - Tso Moriri Lake; 7 - Tianmen Cave; 8 - Dongge Cave; 9 - Qunf Cave, Oman. Background is the June-July-August (JJA) mean 850-hPa isohyet during the period 1971–2000; areas above 3000 m a.m.s.l. are shaded in grey. (C) Monthly average temperature, precipitation and oxygen isotope values from 1986 to 2003 at the Kunming GNIP station (IAEA/WMO).

3. Research methods

3.1. Geochemistry

Total organic carbon (TOC) and total nitrogen (TN), from which carbon/nitrogen (TOC/TN) ratios were calculated, were measured using a VarioEL Cube, Elementar Analysensysteme (GmbH, Germany), after treatment with HCl to remove inorganic carbon from the samples. After combustion in an elemental analyzer (Costech), the carbon isotope composition ($\delta^{13}C$) of bulk organic matter was measured on a continuous-flow gas-ratio mass spectrometer (Finnigan Delta PlusXL) in the environmental isotope laboratory at the University of Arizona. Acetanilide was used as a standard for elemental concentrations, and IAEA-CH-7 and USGS-24 were used as standards for $\delta^{13}C$ measurements. The carbonate $\delta^{18}O$ data reported here are from Hodell et al. (1999), who pretreated sediment samples with H_2O_2 to remove organic matter, prior to analysis using a Micromass PRISM Series II mass spectrometer in the Stable Isotope Laboratory at the University of Florida.

3.2. Pollen analysis and pollen-based temperature reconstruction

Pollen samples were processed following standard procedures (Moore et al., 1991). 1–2 g of sediment were digested with 10% HCl and 40% HF to remove carbonate and SiO_2, respectively, after which the sample was passed through a 10-μm-mesh sieve. At least 500 terrestrial pollen grains were counted per sample and pollen percentages were calculated based on the sum of total terrestrial pollen. The analyses were carried out in the Key Laboratory of Western China's Environmental Systems, Lanzhou University.

A modern calibration set of 1860 surface pollen samples (from an original dataset of 2411 samples), including 355 pollen taxa (Xu et al., 2010; Lu et al., 2011; Zheng et al., 2014), was used, after excluding 551 samples from neighboring countries (Japan, Mongolia and India), from sites influenced by human disturbance (according to field notes), and from tropical and arid regions (Editorial Board of Vegetation of China, 1980). We identified the most significant environmental variable that influenced changes in the fossil pollen assemblages using the randomTF method which was applied to the fossil data and the entire calibration set; then, the range of non-targeted climatic variables (e.g., precipitation) was limited. Based on the gradient of the targeted environmental variable, we chose the weighted-averaging partial least squares (WA-PLS) regression method (ter Braak and Juggins, 1993; Birks et al., 2010; Juggins and Birks, 2012; Chen et al., 2017a) to carry out the reconstruction. All numerical analyses were carried out using the statistical package R (version 3.3.2; R Core Team, 2013). Corresponding analyses were run with the "vegan" library (version 2.4–2; Oksanen et al., 2017); the calibration and regression were run with the "rioja" library (version 0.9–9; Juggins, 2015); and the significance assessments of quantitative reconstructions were run with the "palaeoSig" library (version 1.1–3; Telford and Trachsel, 2015). Detailed information can be found in Chen et al. (2017a).

4. Results

4.1. Sediment records from Xingyun Lake

A puzzling aspect of the sediment record from Xingyun Lake is an apparent hiatus at the beginning of the Holocene (Chen et al., 2014a). We used multiple cores from the lake to address this potential discontinuity. At least seven sediment cores were obtained from Xingyun Lake (Fig. 1A), most of them spanning the period since the late Pleistocene. The first long sediment core (XH-3-IV-89, 8-m-long) was obtained in 1989 from the north basin of the lake using a steel-barreled Livingstone square-rod piston corer. Diatoms were analyzed to infer past changes in lake hydrology and regional environmental changes (Whitmore et al., 1994). In 1994, a 10.2-m-long core (XH-14-X-94) was retrieved from the south basin, from which a bulk carbonate $\delta^{18}O$ record was obtained and used to infer variations in summer monsoon strength during the last ~25,000 yr (Hodell et al., 1999). In 2008, a multi-institution collaborative group obtained three cores from the central and north basins using a UWITEC piston coring system. These three profiles may have lost sediment from the middle sections of the cores, resulting in discontinuous records. Analysis of these cores (XY08A, XYB08 and XY09) produced several publications on changes in regional vegetation and ISM intensity (Chen et al., 2014a, 2014b; Wu et al., 2015b; Hillman et al., 2017), as well as of the changing intensity of human activity in the catchment (Hillman et al., 2014; Wu et al., 2015a). In 2011, a 429-cm-long sediment core was recovered from the western part of the central basin of Xingyun Lake, and multiple variables were analyzed to infer Holocene climatic and environmental changes (Zhang et al., 2014).

Core XY08A has a hiatus at 485 cm spanning the period from 13,600–8500 yr BP (Chen et al., 2014a, 2014b). A similar hiatus was also found in cores XYB08 and XY08C, identified by comparison of records of carbonate content and XRF-determined Ca concentration (Fig. 2). The hiatus in core XYB08 spans the period from ~17,000–8600 yr BP (Aubrey Hillman, personal communication). Chen et al. (2014a) suggested that the hiatus was basin-wide and possibly caused by leakage of water through fissures in the lake bed. There is, however, no dramatic change in carbonate content in core XH-14-X-94 between 700 and 600 cm, and no abrupt shift in carbonate concentration in core XH-3-IV-89. We conclude there was not a hiatus in sedimentation in Xingyun Lake during the late Pleistocene to early Holocene transition and that the dramatic changes in lithology and other sedimentary variables in some cores were caused by the absence of sediments resulting from other factors that are discussed below.

The absence of sediments at some sites may be attributed to erosion by streams. The deepest part of the lake was in the south basin during the late Pleistocene and early Holocene (Fig. S1), and sediments in the shallow north basin could have been eroded by runoff when the lake level was low. More likely, however, sediment was lost during the coring process. Abrupt changes in carbonate content in the three cores occurred at the base of the second drive (the UWITEC piston corer can obtain at most a 3-m-long sediment core in each drive) (Fig. 2), which suggests that sediment was lost during core retrieval. The 'missing' sediment occurs within a lithological transition. During the end of the last glacial, the sediments consisted mainly of grey clay, with a low $CaCO_3$ and organic matter content. During the early to middle Holocene, however, the sediments consisted of carbonate mud with a high organic matter content. The deposits in the upper ~2.5 m of the core (post-1500 yr BP) in the south basin and to ~1.5 m depth in the north basin, consist mainly of red clay with a low carbonate content (Hillman et al., 2014; Wu et al., 2015a). It is possible that the compact clay beneath the loose, low-density carbonate mud was lost during the second drive. We conclude that there was no widespread sedimentation hiatus in Xingyun Lake and that the loss of sediment from several cores occurred during the coring process.

4.2. Depth-age model for the Xingyun Lake sediments

AMS ^{14}C dating of bulk organic matter and gastropod shells was used to develop age models for most of the cores from Xingyun Lake. The exceptions are cores XY08A (Chen et al., 2014a), XYA09 (Hillman et al., 2014) and XYB08 (Hillman et al., 2017) for which age models were reconstructed using AMS ^{14}C dates on charcoal and terrestrial plant macrofossils (wood fragments), which avoids hard-water-lake error (reservoir effects) that can compromise dates from bulk sediments from lakes in areas of carbonate terrain (Hou et al., 2012; Zhou et al., 2015). Whitmore et al. (1994) applied an 1800-yr correction (subtracted), derived from nearby Qilu Lake, to adjust radiocarbon dates from the Xingyun Lake core. Hodell et al. (1999) suggested that dates from Xingyun Lake cores are probably affected by the reservoir effect, similar to other lakes in Yunnan (e.g., Qilu Lake), but they did not apply a correction to the radiocarbon chronology for core XH-14-X-94. Zhang et al. (2014) subtracted 1200 yr from all ages to correct for the reservoir effect, with the assumption that the offset was constant throughout the core. The reservoir effect, however, can differ between lakes and may even change through time within a single lake (Zhou et al., 2015). Zhou et al. (2015) compared the ages of bulk organic matter and terrestrial plant remains from the same depths in both cores XH-14-X-94 and XY08A, and concluded that the radiocarbon reservoir age varied between 960 and 2200 yr during the last 8500 yr at Xingyun Lake.

We generated an integrated chronology, using all reliable sediment dates, by assigning several radiocarbon dates from cores XY08A, XYB08 and XYA09 to equivalent depths in core XH-14-X-94, via stratigraphic correlation of their carbonate content records (Fig. 2). We also obtained two additional AMS ^{14}C dates (Beta-438756 and Beta-438757) from core XH-14-X-94 and one AMS ^{14}C date (LZU047) from core XY08A. These three dates are based on bulk organic matter (Table 1). The radiocarbon date from terrestrial plant remains from 608 to 620 cm in core XY08A is not statistically different with the date from bulk organic matter from 618 to 620 cm, suggesting the reservoir effect at ca. 23,000 yr BP in Xingyun Lake was negligible. In addition, during the late Pleistocene, the carbonate content and TOC content were low and relatively constant, and the amplitude of bulk organic matter $\delta^{13}C$ fluctuations was also low (Fig. S2). These features suggest limited changes to the carbon cycle at Xingyun Lake at that time, and we infer that the reservoir effect during the late Pleistocene was insignificant. The carbonate and TOC contents of the sample from 783 to 785 cm in core XH-14-X-94 are relatively high, indicating a change in the carbon cycle and lake hydrological conditions, with enhanced input of inorganic carbon or pre-aged organic carbon. Thus, it is possible that the carbon reservoir effect affected radiocarbon ages in this part of the core. Combining the work of Whitmore et al. (1994) and Zhou et al. (2015), we used 1800 yr as the reservoir age and subtracted it from the ^{14}C age of bulk sediment sample OS-9089. All 22 dates (Table 1) from the period since the last deglaciation were calibrated to calendar years before present (AD, 1950) using the program CALIB Rev. 7.0, with the IntCal13 calibration data set (Reimer et al., 2013). An age-depth model (Fig. 3) was established using a smoothing spline fit, implemented with the Clam statistical package (Blaauw, 2010) and the statistical software package R. Using the resulting core chronology, temporal patterns in the carbonate $\delta^{18}O$ record from the Xingyun Lake core compare well with those from the $\delta^{18}O$ record in the well-dated Dongge Cave speleothem (Fig. 4E), suggesting the updated age model for core XH-

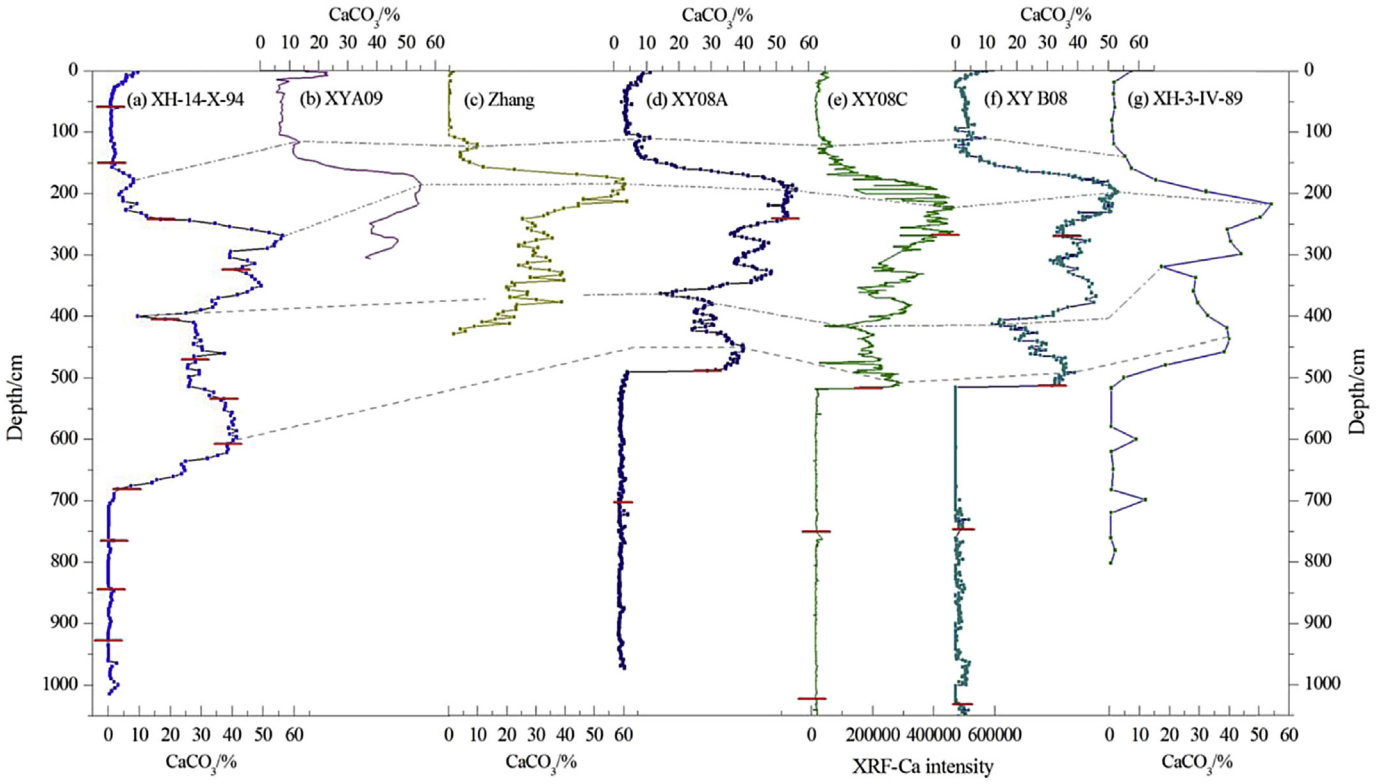

Fig. 2. Comparison of the carbonate content and XRF-Ca intensity in multiple cores from Xingyun Lake. Red bars indicate the base of each recovered section. Dashed lines show correlations between carbonate content records, which enabled radiocarbon dates to be transferred between cores. Citations for studies on cores (a)–(g) are in the legend for Fig. 1A. (For interpretation of the references to colour in this figure legend, the reader is referred to the Web version of this article.)

14-X-94 is reliable.

4.3. Geochemical variables in the Xingyun Lake sediment core during the last 14,000 years

The oxygen isotope composition of bulk carbonates from core XH-14-X-94 ranges from −12‰ to −5‰ VSPDB, with lowest values during the early Holocene (11,000–6500 yr BP) and higher values during the middle to late Holocene, especially after ca. 1500 yr BP. The low sampling resolution used by Hodell et al. (1999) produces apparently abrupt shifts in the $\delta^{18}O$ record. We analyzed additional carbonate isotope samples from the same core to improve the temporal resolution. Relatively larger $\delta^{18}O$ values occurred during the Younger Dryas (YD) (Fig. 4A). Except for the last 1500 yr, $\delta^{18}O$ values from the Xingyun Lake core during the last 14,000 yr show trends similar to those in speleothems from Dongge Cave (Fig. 4E). In addition, the $\delta^{18}O$ record from core XYB09 shows a similar pattern of variation to that in core XH-14-X-94, despite differences in the two core chronologies. The TOC and TN trends are also similar between the two cores during the last 14,000 yr, with relatively low values (mean TOC: 2.6; mean TN: 0.3) during the late Pleistocene. In both records, values increase from the beginning of the Holocene until ~8000 yr BP when they reach maxima; subsequently, they generally decrease, but display several short-term fluctuations at ca. 4000, 1500, and 400 yr BP (Fig. 4B). The carbonate content was low during the late Pleistocene, increased during the Holocene, 'plateaued' during the early Holocene, and then maintained a second interval of high values during the middle to late Holocene. Mean $CaCO_3$ concentrations during the first (10,000–5000 yr BP) and second (5000-1500 yr BP) intervals were 30% and 40%, respectively. The carbonate content decreased abruptly at 1500 yr BP and remained low thereafter (Fig. 4C).

4.4. Pollen in the Xingyun Lake sediment core during the last 14,000 years

4.4.1. Pollen assemblages

The pollen record from Xingyun Lake was generated using two cores. The lower section (~14,000–8500 yr BP) is from core XH-14-X-94, whereas the upper section (since ~8500 yr BP) is from core XY08A. Modern pollen assemblages in 10 surface sediment samples collected throughout Xingyun Lake revealed that the assemblages are similar, regardless of differences in sample location and water depth (Chen et al., 2017b). A total of 78 pollen and spore types were identified in the 71 pollen samples from the Xingyun Lake cores. A summary percentage pollen diagram, with 23 selected taxa, illustrates the main changes in the pollen stratigraphy (Fig. 5). The pollen assemblages are dominated by *Pinus*, with percentages ranging from 29% to ~70%; there is an increasing trend before 11,500 yr BP, a decreasing trend from 11,500–7700 yr BP, and an increasing trend thereafter. Evergreen *Quercus* (hereafter '*Quercus* (E)') is also relatively abundant throughout the entire sequence, with percentages ranging from ~5% to ~30%. Other major pollen types include deciduous *Quercus* (hereafter '*Quercus*'), Poaceae and *Alnus*.

4.4.2. Pollen-based mean July temperature reconstruction

Assessment of the statistical significance of reconstructed climate variables from pollen analysis from the Xingyun Lake cores suggests that MJT was the most important environmental factor influencing the fossil pollen assemblages (Fig. S3). MJT explained more of the variance than did the other three reconstructed variables, as well as >99.9% of the random reconstructions ($p < 0.001$). The calibration data subset, consisting of 549 modern surface pollen samples (Fig. S4), was acquired by limiting the data set to the

Table 1
AMS^{14}C radiocarbon dates from Xingyun Lake.

Core	Sample Lab. no.	Material	Interval in original core (cm)	Composite median depth[a] (cm)	^{14}C age (yr BP)	Error	Calibrated age (Cal yr BP)	Error (1σ)	Reference
XY A09	71481	Wood	35.5	57	110	25	112	50	Hillman et al., 2014
XY A09	71482	Charcoal	37.5	65	110	50	123	45	Hillman et al., 2014
XY A09	71483	Charcoal	59	90	130	25	124	50	Hillman et al., 2014
XY A09	84866	Charcoal	145	237	1060	25	962	20	Hillman et al., 2014
XY B08	141232	Leaf	210.5	279	1785	35	1707	70	Hillman et al., 2017
XY08A	BA120228	Plant remains	226–230	283	1810	30	1760	50	Chen et al., 2014a
XY A09	84867	Wood	250	294	2105	20	2079	40	Hillman et al., 2014
XY A09	84815	Charcoal	263	302	2220	20	2227	75	Hillman et al., 2014
XY B08	141233	Wood	309	320	3065	20	3290	45	Hillman et al., 2017
XY B08	122325	Charcoal	310.5	321	3070	15	3300	40	Hillman et al., 2017
XY08A	BA120229	Plant remains	294–306	322	3130	30	3330	60	Chen et al., 2014a
XY B08	141234	Charcoal	408.5	398	4080	20	4564	30	Hillman et al., 2017
XY08A	BA120230	Plant remains	376–378	421	5105	25	5835	75	Chen et al., 2014a
XY B08	172626	Leaf	446.5	463	5665	20	6444	20	Hillman et al., 2017
XY08A	BA120231	Plant remains	410–412	485	5785	25	6595	40	Chen et al., 2014a
XY08A	BA120241	Charcoal	436–438	523	6715	35	7570	45	Chen et al., 2014a
XY B08	141235	Leaf	504.5	610	7375	35	8200	50	Hillman et al., 2017
XY08A	BA120232	Plant remains	476–478	615	7535	30	8365	20	Chen et al., 2014a
XY08A	Beta - 333693	Plant remains	484–486	621	7720	40	8495	45	Chen et al., 2014a
XH-14-X-94	OS-9089	Bulk organic matter	783–785	635	9680	45	11045	150	Hodell et al., 1999
XH-14-X-94	Beta - 438756	Bulk organic matter	860–863	692	10540	30	12500	65	This study
XH-14-X-94	Beta - 438757	Bulk organic matter	917–919	748	12290	40	14195	90	This study
XY08A[b]	BA120234	Plant remains	608–620	NA	23150	80	27440	90	Wu et al., 2015b
XY08A[b]	LZU047	Bulk organic matter	618–620	NA	23250	130	27510	110	This study

[a] Median depths of radiocarbon dates in each interval were transferred to depths in core XH-14-X-94 based on correlation between the records of carbonate content.
[b] Dates used to evaluate the carbon reservoir effect.

precipitation range of 550–1500 mm. The WA-PLS method was chosen for establishing regression and calibration functions and was used to generate MJT reconstructions from the stratigraphic pollen data. The proportions of the variance explained by the MJT reconstructions are higher than those when the whole calibration set was used. In addition, conventional statistics (Table S1) showed that the calibration data subset has a good level of performance, as indicated by high R^2 and low RMSEP (Birks, 1998). Precipitation is not the most significant factor influencing the fossil pollen assemblages, even before limiting the precipitation gradient (Fig. S3A).

Quercus (E) is grouped into drought-resistant broadleaved trees which can generally tolerate dry conditions (Jarvis, 1993), and increased abundances of *Quercus (E)* pollen from lacustrine sediments in southwest China are attributed to enhanced aridity (e.g., Shen et al., 2006; Chen et al., 2014b) which can be caused by decreased precipitation and increased temperature. The roughly similar trend of *Quercus (E)* pollen content and the reconstructed MJT further supports the reliability of the reconstruction. The pollen-based temperature reconstruction (Fig. 4D) reveals an increasing trend of MJT before 12,500 yr BP and a decrease during the YD (~12,500–11,500 yr BP). In the beginning of the Holocene, MJT increased slowly and reached relatively high values around 8000 yr BP. The values remained high during the interval from 8000 to 5500 yr BP, but decreased thereafter.

5. Discussion

5.1. Holocene summer temperature variations in southwest China

Summer temperatures (MJT) at Xingyun Lake in the late glacial were low, increased during the early Holocene, were highest during the middle Holocene, and then decreased during the late Holocene (Fig. 6D). The range of inferred values was 21.0–26.5 °C. The pollen-inferred temperature derived from surface samples (21.2 °C), is close to the modern instrumental July temperature in Kunming (22 °C), supporting the reliability of reconstructions from down-core pollen assemblages. Previous studies cautioned that pollen-based summer temperature inferences are affected by other variables, such as winter temperature, precipitation, or even non-climatic factors (Birks et al., 2010; Li et al., 2015a). In this study, however, we used a novel approach to reconstruct paleoclimate quantitatively. It relies on identifying the environmental variable that is most significant in controlling the fossil pollen assemblage and limits the modern ranges of other environmental variables.

TOC and TN reflect the paleoproductivity of lakes and lake catchments (Meyers and Lallier-Vergès, 1999). The TOC/TN ratio of lake sediments is indicative of the relative amounts of organic matter derived from terrestrial inputs versus aquatic macrophytes and algae. The ratio from Xingyun Lake indicates contributions from both sources (Fig. S5). To further distinguish organic matter derived from terrestrial versus aquatic sources, we used the *n*-alkane record of Zhou et al. (2015). Zhou et al. (2015) reported that *n*-alkanes in later early-Holocene and middle Holocene sediment from Xingyun Lake were dominated by long carbon chain lengths (C_{27}-C_{31}), which are typically derived from the leaf waxes of terrestrial vascular plants (Ficken et al., 2000) (Fig. S5). Similarity between the records of organic matter $\delta^{13}C$ and atmospheric CO_2 concentrations (Fig. S5) indicates that the plants that supplied organic matter (OM) to the Xingyun Lake sediments grew in an environment with rapid and complete CO_2 exchange, and that organic matter in early Holocene sediments may have had the same sources as OM in the middle Holocene sediments. Therefore, we conclude that the OM in the Xingyun Lake sediments during the early to middle Holocene was derived mainly from terrestrial inputs.

It is generally assumed that rainfall and temperature are positively correlated on seasonal time scales in monsoonal Asia. Thus, previous studies have used the TOC content of lake sediments as an indicator of precipitation amount in the region (An et al., 2011, 2012), because higher temperature and greater precipitation promote increased biomass in lake catchments. However, whether this seasonal relationship can be scaled up to the entire Holocene needs to be carefully evaluated. For instance, a study of Holocene TOC

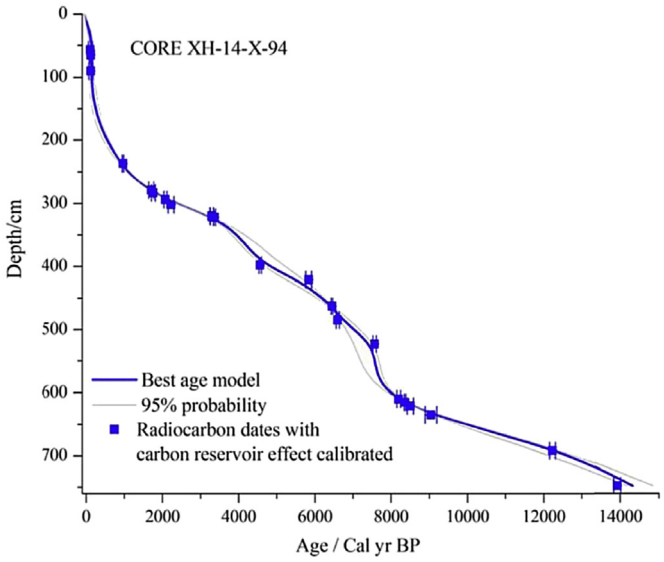

Fig. 3. Radiocarbon dates with 1-sigma error bars and a smoothing spline age model with 95% confidence intervals for core XH-14-X-94 from Xingyun Lake.

accumulation in the sediment of 58 lakes throughout China indicated a generally increasing accumulation trend since 12,000 yr BP in most lakes (Wang et al., 2015). This TOC accumulation trend tracks simulated global temperature (Liu et al., 2014), but differs from the trend seen in sediment records from lakes in the ISM (Fleitmann et al., 2003; Dykoski et al., 2005) and East Asian summer monsoon regions (Chen et al., 2015). We conclude that changes in the TOC content of the Xingyun Lake sediments mainly result from temperature variations and that high summer temperatures promote high biomass in both terrestrial and lake systems. The low but increasing early Holocene biomass and high middle Holocene biomass in Xingyun Lake mainly reflects a middle Holocene summer thermal maximum.

We also compared our inferred summer temperature inferences with other summer temperature reconstructions from the ISM region. A quantitative summer (mean July) temperature reconstruction inferred from subfossil chironomids in Tiancai Lake, Yunnan Province, together with variations in the abundance of the diatom *Aulacoseira alpigena* and *Tsuga* forest from the same catchment, suggested that summers were cooler during the period 11,800–10,500 yr BP, and that summer temperature subsequently increased, with fluctuations, before reaching high values during the interval from 8500 to 6000 yr BP. After ca. 5500 yr BP, the reconstructed summer temperature generally decreased (Zhang et al., 2017a). This pattern of temperature change resembles that of our pollen-based summer (mean July) temperature record.

5.2. ISM precipitation recorded in carbonate oxygen isotope ($\delta^{18}O$) records

5.2.1. Environmental significance of lacustrine carbonate $\delta^{18}O$ values

The boundary between the Pleistocene and the Holocene recorded in Xingyun Lake is characterized by an abrupt change in carbonate content, with low values during the late Pleistocene and high values during the warmer and wetter early Holocene. Because carbonate and OM concentrations are positively correlated during the Holocene (Fig. 4B and 4C), primary productivity and carbonate precipitation at Xingyun Lake were apparently linked during the Holocene, as suggested by Hodell et al. (1999). X-ray diffraction analysis identified calcite as the primary carbonate mineral in surface sediments and core samples from Xingyun Lake (Zhang et al., 2003; Hillman et al., 2014). Scanning electron microscope (SEM) results showed that the calcite has a euhedral structure, indicating that it was precipitated from the water column (i.e., authigenic) (Hillman et al., 2017). Samples from core XH-14-X-94 used for isotopic analysis consisted of bulk carbonate, which may include both biogenic (autochthonous) material and detrital (allochthonous) carbonate. The $\delta^{18}O$ record from bulk carbonate displays the same stratigraphic pattern as that for the fine-grained carbonate (<63 μm fraction) (Fig. 4A), indicating there is minimal non-authigenic calcite in the sediments. These several lines of evidence demonstrate that carbonates in the sediments of Xingyun Lake are authigenic calcite whose oxygen and carbon isotope compositions can be used to infer climatic and hydrological variations in the lake catchment.

The $\delta^{18}O$ of authigenic calcite is determined by the temperature and $\delta^{18}O$ of the water from which it precipitates (Craig, 1965; Leng and Marshall, 2004). Hodell et al. (1999) and Hillman et al. (2014) measured calcite $\delta^{18}O$ in surface sediments from Xingyun Lake and obtained results very close to expected values calculated using modern lake water temperature and $\delta^{18}O$. This supports the claim that the calcite is authigenic and that it precipitates in isotopic equilibrium with the lake water. The temperature-dependent equilibrium isotopic fractionation between carbonate and water is approximately −0.24‰ per℃ (Craig, 1965), and the large range of variability (~7‰) in the oxygen isotopic composition of authigenic calcite in Xingyun Lake during the Holocene was thus controlled only to a limited extent by temperature. For example, if the calcite $\delta^{18}O$ values were controlled exclusively by temperature, it would imply a range of past temperatures on the order of 28 °C. It is a far more reasonable explanation that the variations in calcite $\delta^{18}O$ were controlled mainly by fluctuations in the oxygen isotopic composition of the lake water, which in turn was governed by the $\delta^{18}O$ of precipitation, and evaporation from the lake surface, related to temperature (Zhang et al., 2011a; Leng and Marshall, 2004).

Precipitation in Yunnan Province is derived mainly from moisture transported from low-latitude oceans (Fig. 1A; An et al., 2011). Changes in the isotopic composition of source waters are linked to hydrological conditions in the source regions and to deglaciation, the latter having caused a decrease of ~0.5‰ in seawater $\delta^{18}O$ during the first half of the Holocene (Edwards et al., 2003; Dykoski et al., 2005). Hillman et al. (2014) compared the relationship between δD and $\delta^{18}O$ in modern lake water with values for the global meteoric water line, and found that Xingyun Lake apparently loses substantial water to evaporation. Therefore, more negative $\delta^{18}O$ values of the Xingyun Lake water results from increased input of ^{18}O-depleted water and/or reduced evaporation. Although evaporation does influence the lake water isotope values to some extent today, Xingyun Lake was hydrologically open, with a substantial outflow to the Gehe River, at least during the early Holocene (Hillman et al., 2017); thus there was continual water replacement by runoff and groundwater inflow. In addition, after calculating early Holocene theoretical calcite $\delta^{18}O$ values, it was found that the assumed results are quite close to observed values (Hillman et al., 2017). We surmise that evaporation effects had minimal impact on the isotope mass balance of the water body during the early Holocene. For the middle to late Holocene, a decrease of the precipitation/evaporation balance may have been caused by a weakening of precipitation and the enrichment of evaporation (Hillman et al., 2017). However, the influences of temperature and evaporation on the isotopic composition of the lake water were probably relatively small compared to the 4‰ range observed in the calcite $\delta^{18}O$ record from ca. 7000-1500 yr BP, which is similar to the speleothem $\delta^{18}O$ record (e.g., Wang et al., 2005). Thus, the variations in

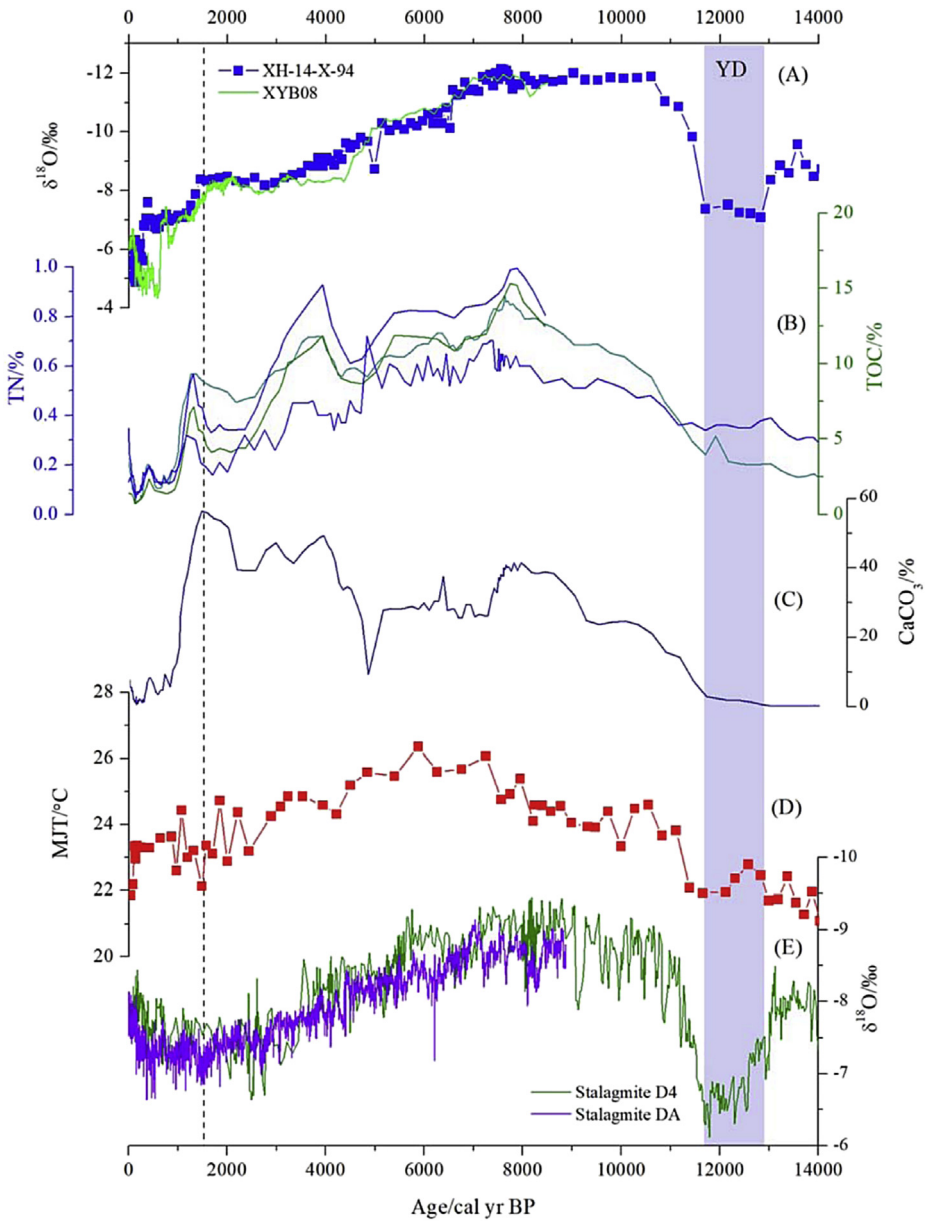

Fig. 4. Multiple variables in the Xingyun Lake sediment and their comparison with the speleothem $\delta^{18}O$ record from Dongge Cave. (A) Lacustrine carbonate $\delta^{18}O$ records from Xingyun Lake; green line is the record from core XYB08 (Hillman et al., 2017) and the blue line with squares is from core XH-14-X-94 (Hodell et al., 1999); (B) TOC (green) and TN (blue) records from cores XH-14-X-94 (long record) and XY08A (short record); (C) carbonate content of core XH-14-X-94 (Hodell et al., 1999); (D) pollen-based mean July temperature (MJT) reconstruction from Xingyun Lake; (F) speleothem (D4 and DA) oxygen isotope records from Dongge Cave (Dykoski et al., 2005; Wang et al., 2005). The vertical bar indicates the YD event and the dashed line represents the onset of increasing human activity in the catchment (Wu et al., 2015a). (For interpretation of the references to colour in this figure legend, the reader is referred to the Web version of this article.)

carbonate $\delta^{18}O$ of Xingyun Lake were dominated by variations in the isotopic composition of precipitation.

Modern observations show that the $\delta^{18}O$ of precipitation in the ISM region is dominated by the summer rainfall amount effect (Tian et al., 2001; Yu et al., 2008): namely, $\delta^{18}O$ values become more negative as rainfall increases. Over a period of ~30 years, linear correlation between weighted-average annual $\delta^{18}O$ of precipitation and yearly precipitation amount at four stations in the ISM region was negative overall (Li et al., 2015b). On long timescales, e.g. over the Holocene, the speleothem $\delta^{18}O$ records from the ISM regions have been widely accepted as reflecting ISM intensity or precipitation amount (Fleitmann et al., 2003, 2007; Dykoski et al., 2005). Given the large seasonal range in the $\delta^{18}O$ of rainfall related to the monsoon (~10‰ at Kunming), the $\delta^{18}O$ of the lake water is sensitive to changes in the seasonal distribution and amount of rainfall. Moreover, the $\delta^{18}O$ of the Xingyun Lake water would have decreased because of the greater contributions of ^{18}O-depleted rainfall to the lake. Thus, long-term variability in the carbonate $\delta^{18}O$ record from Xingyun Lake should reflect the intensity of ISM precipitation and relatively low $\delta^{18}O$ values from 11,000–6500 yr BP indicate that higher summer precipitation occurred during that interval.

5.2.2. Carbonate oxygen isotope records from ISM-dominated regions since the late glacial

Previous research showed that tracking monsoon precipitation changes on the Asian continent using the stable isotope composition of authigenic lacustrine carbonates is feasible (Wei and Gasse,

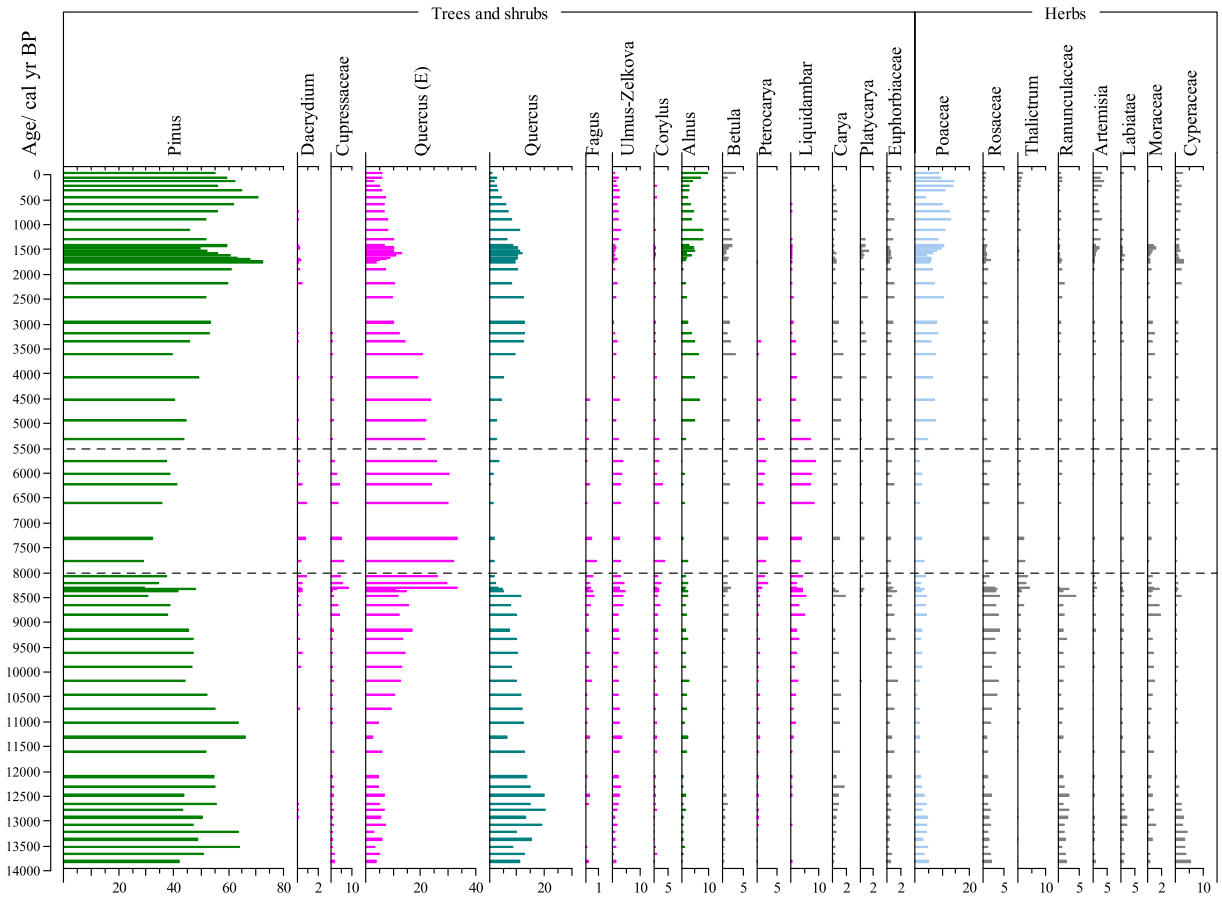

Fig. 5. Pollen diagram from Xingyun Lake.

1999). For instance, the southern Tibetan Plateau was shown to be an area influenced by the ISM (Yao et al., 2012) and several studies of $\delta^{18}O$ in lacustrine carbonates were completed over the past several decades (e.g., Fig. S6). For example, Selin Co (Co means Lake) had high $\delta^{18}O$ values during the late Pleistocene, suggesting a lower lake level. Generally lower, but slowly increasing $\delta^{18}O$ values during the early Holocene reflect a relatively stable water level with a balance between inflow and evaporation (Morinaga et al., 1993). Early Holocene wet conditions were also inferred from relatively lower $\delta^{18}O$ values in Bangong Co, and attributed primarily to an increase in summer monsoon precipitation (Gasse et al., 1996; Hou et al., 2017). The $\delta^{18}O$ record from Tso Moriri Lake in the NW Himalayas shows substantial variability during the Late glacial and lower values during the early Holocene (11,200–8500 yr BP), suggesting fluctuating conditions and a maximum in ISM precipitation, respectively (Mishra et al., 2015). A persistent enrichment trend during the late Holocene indicates declining monsoon precipitation (Mishra et al., 2015). Qilu Lake lies south of Xingyun Lake and its carbonate oxygen isotope record displays low $\delta^{18}O$ values from 11,500–7000 yr BP, which reflects the high intensity of the summer (southwest) Asian monsoon during the early Holocene (Hodell et al., 1999). In summary, lacustrine authigenic carbonate $\delta^{18}O$ records from the ISM region appear to document the intensity of monsoon precipitation, with highest monsoon precipitation during the early Holocene.

Speleothems are invaluable paleoclimate archives because they can often be dated accurately and at high resolution, although the environmental significance of the stalagmite $\delta^{18}O$ record is debated (Maher, 2008; Tan, 2014; Clemens et al., 2010; Pausata et al., 2011; Caley et al., 2014; Liu et al., 2015). Speleothem $\delta^{18}O$ values from the East Asian summer monsoon region cannot be used as an indicator of regional summer monsoon precipitation intensity (Liu et al., 2017). In the ISM region, however, lower $\delta^{18}O$ values usually reflect greater precipitation (Fleitmann et al., 2003). A speleothem from Tianmen Cave, on the southern Tibetan Plateau (Fig. 1B), provided a detailed record of variations in precipitation $\delta^{18}O$ from 9100 to 4300 yr BP (Cai et al., 2012). In the core region of the ISM, the $\delta^{18}O$ record from Qunf Cave, Oman, faithfully reflects the amount of ISM precipitation (Fleitmann et al., 2003). The $\delta^{18}O$ values from Dongge Cave decreased dramatically at the start of the Holocene and remained low until 6000 yr BP (Dykoski et al., 2005). The above records all indicate strong monsoon precipitation during the early Holocene, and a decrease in monsoon precipitation during the middle to late Holocene, characterized by an abrupt shift to greater $\delta^{18}O$ values.

5.3. Decoupled summer temperature and monsoon precipitation in southwest China

Today, seasonal temperature differences at Xingyun Lake are strongly correlated with summer monsoon precipitation amount (Fig. 1C). Modeling studies, however, indicate that this relationship cannot be scaled upwards to orbital timescales (Kutzbach et al., 2008; Ziegler et al., 2010). On such long timescales, the dearth of paleoclimate records that provide independent measures of temperature and precipitation from the same sites limits our understanding of Holocene climate variability in monsoonal Asia. Both records of temperature and precipitation in our study come from

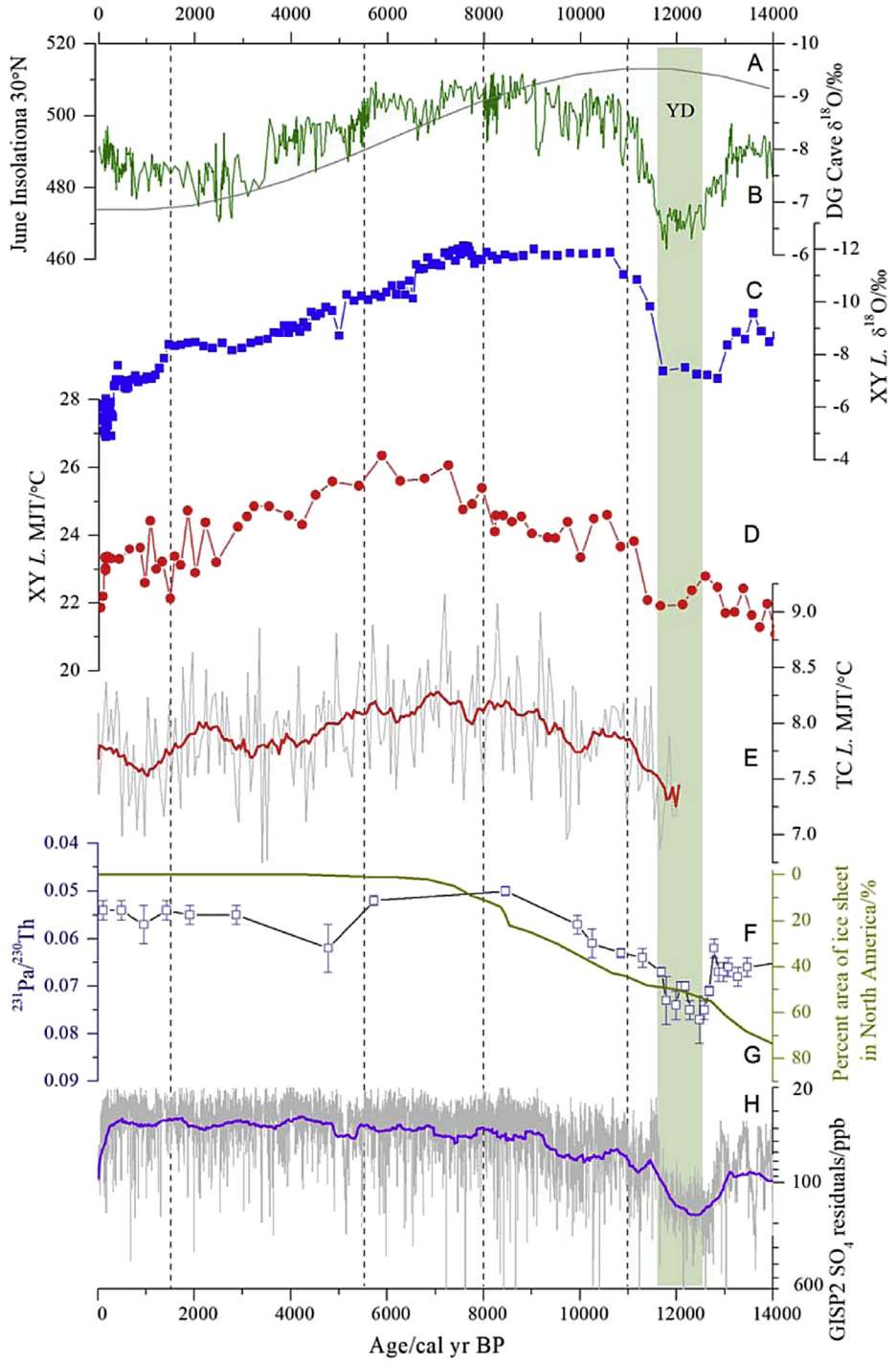

Fig. 6. Dynamics of the decoupled early Holocene summer monsoon precipitation and temperature variations in southwest China. (A) June solar insolation at 30° N (Berger and Loutre, 1991); (B) speleothem $\delta^{18}O$ record from Dongge Cave (Dykoski et al., 2005); (C) carbonate $\delta^{18}O$ record from Xingyun Lake (Hodell et al., 1999), with a new age model; (D) pollen-based mean July temperature reconstruction from Xingyun Lake; (E) summer temperature reconstruction based on subfossil chironomids from Tiancai Lake, Yunnan Province (Zhang et al., 2017a); (F) squares indicate $^{231}Pa/^{230}Th$ ratios from core GGC5 from the North Atlantic, with ages based on ^{232}Th activity (Mcmanus et al., 2004), and the yellow-green line represents the percentage area of ice the sheet in North America (Dyke, 2004); (G) percentage area of ice sheets in North America (Dyke, 2004); (H) SO_4 residuals from the GISP2 ice core, Greenland (Zielinski and Mershon, 1997). (For interpretation of the references to colour in this figure legend, the reader is referred to the Web version of this article.)

the same sediment core and thus they have a common age model, and this enables us to assess the timing and magnitude of changes in summer temperature and monsoon precipitation intensity (the $\delta^{18}O$ record), while controlling for errors associated with age-model uncertainties.

Initial comparison of our temperature and precipitation records at the glacial/interglacial timescale indicates that temperature and monsoon precipitation were similar, both displaying low values during the late Pleistocene and higher values during the Holocene (Fig. 6B and C), suggesting they were driven largely by the same

controlling factors. There was, however, a decoupling of summer temperature (MJT) and monsoon precipitation intensity during the early Holocene, specifically during the period from 10,700–5500 yr BP. During the first half of the interval (10,700–8000 yr BP), summer temperature increased gradually, whereas precipitation had reached its maximum. During the second half of the interval (8000-5500 yr BP), summer temperature reached high values while precipitation commenced a decreasing trend. The MJT record shows a middle Holocene maximum, which is at odds with the carbonate $\delta^{18}O$ record from the same core, the latter exhibiting a pattern of variation similar to the speleothem $\delta^{18}O$ record from Dongge Cave (Fig. 6A). Both $\delta^{18}O$ records indicate that highest precipitation occurred during the early Holocene. We therefore propose that variations in summer temperature and precipitation in southwest China were decoupled during the early Holocene.

The validity of this finding largely depends on the reliability of the reconstructed precipitation and temperature records. Although there are records showing a wet middle Holocene in southwest China (e.g., Xiao et al., 2014), this pollen-based evidence lacks a quantitative basis. In addition, the timing of the ISM onset during the early Holocene remains controversial. An early ISM onset at ~11,400 yr BP has been proposed (e.g., Overpeck et al., 1996), as well as a later ISM onset at ~10,000 yr BP (e.g., Schulz et al., 1998; Fleitmann et al., 2007). Moreover, a two-step development of the ISM during the early Holocene was reconstructed from a lake in the central Tibetan Plateau (He et al., 2017). Considering the potential dating error, all of these records illustrate an early Holocene ISM maximum.

The stacked global annual temperature record of Marcott et al. (2013) displays a maximum in the early Holocene, with a temperature plateau extending from 9500 to 5500 yr BP, followed by a cooling trend through the middle to late Holocene (5500-100 yr BP), highlighting the importance of boreal summer insolation for Holocene temperature in northern, high-latitude regions. This stacked temperature record, however, is contradicted by a climate simulation study, which suggests that the trend in the stacked record was imparted mainly by several alkenone-based sea surface summer temperature records from the Northern Hemisphere (Liu et al., 2014). In China, the interval of greatest Holocene warmth is traditionally thought to have occurred during the Middle Holocene Optimum, roughly from 8500 to 3000 ^{14}C yr BP, with higher-than-present annual average temperatures across the whole of China (Shi et al., 1993). Nevertheless, using output from 36 climate models in the Paleoclimate Modeling Intercomparison Project (PMIP), Jiang et al. (2012) found that 35 of those models yielded colder-than-present (i.e., preindustrial) annual temperatures over China during the middle Holocene, ca. 6000 yr BP. The simulation results also indicate that in all the PMIP models, temperature increased in summer during the middle Holocene, closely tracking changes in solar radiation received at the top of the atmosphere over China. Jiang et al. (2012) argued that the simulated low annual temperature over China was caused by low annual total solar insolation during the middle Holocene. Therefore, the inconsistency between proxy-based paleotemperature reconstructions and simulation results demonstrates the need to further explore seasonal temperature variations and the forcing factors, including internal feedbacks that include vegetation type, cloud cover, and ice volume conditions, as well as orbital-scale insolation changes.

Large variations in summer insolation at northern, high latitudes drove climate transitions from cold glacial periods to warmer and wetter interglacials, such as the Holocene (Tzedakis et al., 2012). The decreasing trend in summer insolation during the Holocene in the Northern Hemisphere (Berger and Loutre, 1991) led to a gradual decrease in the ISM. Summer temperature (MJT) and monsoon precipitation ($\delta^{18}O$) decreased together after ~5500 yr BP because of the decrease in summer insolation; summer temperature in Yunnan during the early Holocene, however, did not track the summer insolation trend closely, and there was evidently a time lag. It has been suggested that high-latitude regions are more sensitive to summer insolation changes because a high percentage of their area consists of continental landmass. At lower latitudes, the ratio of continental landmass to ocean is relatively lower, and thus, temperature in these regions is potentially modified by the interaction between the ocean and atmosphere (Marcott et al., 2013).

From 1960 to 2005, total cloud cover decreased over southwest China, including Yunnan Province (Zhang et al., 2011b). In addition, a study of temperature and precipitation variations in Yunnan Province during the period from 1961 to 2007, based on data from meteorological stations, found that mean annual precipitation, especially summer precipitation, decreased substantially, whereas summer temperature increased (Liu et al., 2010). This negative relationship between cloud cover and summer temperature was also found in India during the period 1931–2002 (Roy and Balling, 2005). Because of increasing anthropogenic emissions of CO_2 and aerosols during the past several decades, the relationship between precipitation, temperature and cloud cover has become more complicated; however, it is clear that rainfall is derived from clouds and that increased rainfall requires increased cloudiness, irrespective of the timescale. Unfortunately, there are no reliable long time-series of cloud cover variability for southwest China. Simulation results show that precipitation and cloud cover increased during the middle Holocene in northern China, while they both decreased in southern China (Liu et al., 2009). This type of middle Holocene precipitation model for eastern China was reconstructed from paleoclimate records (Xie et al., 2013; Chen et al., 2015). Strong early Holocene monsoon precipitation in southwest China should have resulted from an enhanced cloud cover in the region. The radiative effect of clouds has attracted increasing attention; for example, it was found that decreasing cloud cover drives the recent loss of mass from the Greenland ice sheet by enhancing the melt-albedo feedback (Hofer et al., 2017). Thus, enhanced albedo effect from increasing cloud cover in southwest China during the early Holocene could have caused a reduction in summer temperature.

Other factors may have influenced the evolution of climate in southwest China since the last deglaciation. For example, during the YD cold period, the strength of the Atlantic Meridional Overturning Circulation (AMOC) weakened, as indicated by $^{231}Pa/^{230}Th$ ratios in North Atlantic deep-sea sediments (Fig. 6F; Mcmanus et al., 2004). Moreover, the decreased monsoon precipitation and summer temperature inferred from our records indicate a response to North Atlantic cooling. Significantly, sediment records from the Arabian Sea indicate a close link between the Indian monsoon system and abrupt climate changes in the North Atlantic region during both the last glacial (Deplazes et al., 2013) and the Holocene (Gupta et al., 2003). The Laurentide ice sheet persisted into the early Holocene (Fig. 6G; Dyke, 2004), which sustained the regional albedo and continuously supplied meltwater to the North Atlantic. These climate influences from high northern latitudes potentially influenced summer temperature in the ISM region via ocean-atmosphere interactions. In addition, the relatively high concentration of atmospheric aerosols, indicated by the insoluble microparticle record of the GISP2 (Greenland) ice core (Zielinski and Mershon, 1997, Fig. 6H) during the early Holocene, could have weakened summer insolation by radiative feedbacks (e.g., Liu et al., 2018).

6. Conclusions

We compiled paleoclimate records and radiocarbon dates from

sediment cores collected in Xingyun Lake, Yunnan Province, southwest China, and we produced a robust chronology and reliable paleoclimate inferences for the interval from the last glacial termination to the present. The record enabled us to produce continuous composite summer temperature and monsoon precipitation records, which we used to determine whether precipitation and temperature responded directly to orbital forcing, with no phase lag, or whether the response was delayed substantially by internal feedback forcings. Pollen assemblages were used to reconstruct climate quantitatively, using modern calibration datasets and transfer functions. Because mean July temperature (MJT) captures most of the long-term variability in fossils pollen records, we reconstructed MJT, which ranged from 21.0 to 26.5 °C, over the past 14,000 yr. Low, but increasing MJT occurred during the early Holocene; high values characterized the middle Holocene (8000-5500 yr BP); and there was a decreasing MJT trend during the late Holocene. An authigenic calcite $\delta^{18}O$ record from the same lake shows relatively lower values during the early Holocene (11,000–6500 yr BP), indicating strong monsoon precipitation. We therefore suggest that summer temperature and precipitation in southwest China during the early Holocene were decoupled. We propose that the albedo effect of enhanced cloud cover during the early Holocene depressed summer temperatures. In addition, the North American ice sheets and high atmospheric aerosol concentrations may also have suppressed summer temperatures during the early Holocene.

Acknowledgments

We sincerely thank two anonymous reviewers for their valuable comments and suggestions, and we thank Dr. Jan Bloemendal for English improvement. This research was supported by the General Financial Grant (Grant No. 2017M623272) from the China Postdoctoral Science Foundation, the International Partnership Program of Chinese Academy of Sciences (Grant No. 131C11KYSB20160061) and the Fundamental Research Funds for the Central Universities (Grant No. lzujbky-2018-it73).

Appendix A. Supplementary data

Supplementary data related to this article can be found at https://doi.org/10.1016/j.quascirev.2018.05.038.

References

An, Z.S., Clemens, S.C., Shen, J., Qiang, X.K., Jin, Z.D., Sun, Y.B., Prell, W.L., Luo, J.J., Wang, S.M., Xu, H., Cai, Y.J., Zhou, W.J., Liu, X.D., Liu, W.G., Shi, Z.G., Yan, L.B., Xiao, X.Y., Chang, H., Wu, F., Ai, L., Lu, F.Y., 2011. Glacial-interglacial Indian summer monsoon dynamics. Science 333 (6043), 719–723.

An, Z.S., Colman, S.M., Zhou, W.J., Li, X.Q., Brown, E.T., Jull, A.J.T., Cai, Y.J., Huang, Y.S., Lu, X.F., Chang, H., Song, Y.G., Sun, Y.B., Xu, H., Liu, W.G., Jin, Z.D., Liu, X.D., Cheng, P., Liu, Y., Ai, L., Li, X.Z., Liu, X.J., Yan, L.B., Shi, Z.G., Wang, X.L., Wu, F., Qiang, X.K., Dong, J.B., Lu, F.Y., Xu, X.W., 2012. Interplay between the westerlies and Asian monsoon recorded in Lake Qinghai sediments since 32 ka. Sci. Rep. 2 (8), 619.

Berger, A., Loutre, M.F., 1991. Insolation values for the climate of the last 10 million years. Quat. Sci. Rev. 10, 297–317.

Birks, H.J.B., 1998. Numerical tools in palaeolimnology-Progress, potentialities, and problems. J. Paleolimnol. 20, 301–332.

Birks, H.J.B., Heiri, O., Seppä, H., Bjune, A.E., 2010. Strengths and weaknesses of quantitative climate reconstructions based on late-Quaternary biological proxies. Open Ecol. J. 3, 68–110.

Blaauw, M., 2010. Methods and code for 'classical' age modeling of radiocarbon sequences. Quat. Geochronol. 5 (5), 512–518.

Cai, Y.J., Zhang, H.W., Cheng, H., An, Z.S., Edwards, R.L., Wang, X.F., Tan, L.C., Liang, F.Y., Wang, J., Kelly, M., 2012. The Holocene Indian monsoon variability over the southern Tibetan plateau and its teleconnections. Earth Planet Sci. Lett. 335–336 (3), 135–144.

Caley, T., Roche, D.M., Renssen, H., 2014. Orbital Asian summer monsoon dynamics revealed using an isotope-enabled global climate model. Nat. Commun. 5, 5371.

Chen, F.H., Chen, X.M., Chen, J.H., Zhou, A.F., Wu, D., Tang, L.Y., Zhang, X.J., Huang, X.Z., Yu, J.Q., 2014a. Holocene vegetation history, precipitation changes and Indian summer monsoon evolution documented from sediments of Xingyun Lake, southwest China. J. Quat. Sci. 29 (7), 661–674.

Chen, F.H., Xu, Q.H., Chen, J.H., Birks, H.J.B., Liu, J.B., Zhang, S.R., Jin, L.Y., An, C.B., Telford, R.J., Cao, X.Y., Wang, Z.L., Zahng, X.J., Selvaraj, K., Lü, H.Y., Li, Y.C., Zheng, Z., Wang, H.P., Zhou, A.F., Dong, G.H., Zhang, J.W., Huang, X.Z., Bloemendal, J., Rao, Z.G., 2015. East Asian summer monsoon precipitation variability since the last deglaciation. Sci. Rep. 11186.

Chen, J.H., Lv, F.Y., Huang, X.Z., Birks, H.J.B., Telford, R.J., Zhang, S.R., Xu, Q.H., Zhao, Y., Wang, H.P., Zhou, A.F., Huang, W., Liu, J.B., Wei, G.Y., 2017a. A novel procedure for pollen-based quantitative paleoclimate reconstructions and its application in China. Sci. China Earth Sci. https://doi.org/10.1007/s11430-017-9095-1.

Chen, X.M., Chen, F.H., Zhou, A.F., Huang, X.Z., Tang, L.Y., Wu, D., Zhang, X.J., Yu, J.Q., 2014b. Vegetation history, climatic changes and Indian summer monsoon evolution during the Last Glaciation (36400-13400 cal yr BP). Palaeogeogr. Palaeoclimatol. Palaeoecol. 410, 179–189.

Chen, X.M., Huang, X.Z., Wu, D., Zhang, X.N., Dodson, J., Zhou, A.F., Chen, F.H., 2017b. Modern pollen assemblages in topsoil and surface sediments of the Xingyun Lake catchment, central Yunnan Plateau, China, and their implications for interpretation of the fossil pollen record. Rev. Palaeobot. Palynol. 241, 1–12.

Clemens, S.C., Prell, W.L., Sun, Y.B., 2010. Orbital-scale timing and mechanisms driving Late Pleistocene Indo-Asian summer monsoons: reinterpreting cave speleothem $\delta^{18}O$. Paleoceanography 25 (PA4207), 545–558.

Cook, C.G., Jones, R.T., Turney, C.S.M., 2013. Catchment instability and Asian summer monsoon variability during the early Holocene in southwestern China. Boreas 42 (1), 224–235.

Craig, H., 1965. The measurement of oxygen isotope palaeotemperatures. In: Tongiorgi, E. (Ed.), Stable Isotopes in Oceanographic Studies and Palaeotemperatures. Consiglio Nazionale delle Ricerche Laboratorio di Geologia Nucleare, Pisa.

Deplazes, G., Lückge, A., Peterson, L.C., Timmermann, A., Hamann, Y., Hughen, K.A., Röhl, U., Laj, C., Cane, M.A., Sigman, D.M., Haug, G.H., 2013. Links between tropical rainfall and North Atlantic climate during the last glacial period. Nat. Geosci. 6 (3), 213–217.

Dyke, A.S., 2004. An outline of North American Deglaciation with emphasis on central and northern Canada. Dev. Quat. Sci. 2, 373–424.

Dykoski, C.A., Edwards, R.L., Cheng, H., Yuan, D.X., Cai, Y.J., Zhang, M.L., Lin, Y.S., Qing, J.M., An, Z.S., Revenaugh, J., 2005. A high-resolution, absolute-dated Holocene and deglacial Asian monsoon record from Dongge Cave, China. Earth Planet Sci. Lett. 233 (1–2), 71–86.

Editorial Board of Yunnan Vegetation in China, 1987. Vegetation of Yunnan Province. Science Press, Beijing (in Chinese).

Edwards, R.L., Gallup, C.D., Cheng, H., 2003. Uranium-series dating of marine and lacustrine carbonates. In: Bourdon, B., Henderson, G.M., Lundstrom, C.C., Turner, S.P. (Eds.), Uraniumseries Geochemistry, vol. 52. Mineralogical Society of America, Washington, DC, pp. 364–405.

Ficken, K.J., Li, B., Swain, D.L., Eglinton, G., 2000. An n-alkane proxy for the sedimentary input of submerged/floating freshwater aquatic macrophytes. Org. Geochem. 31, 745–749.

Fleitmann, D., Burns, S.J., Mudelsee, M., Neff, U., Kramers, J., Mangini, A., Matter, A., 2003. Holocene forcing of the Indian monsoon recorded in a stalagmite from southern Oman. Science 300 (5626), 1737–1739.

Fleitmann, D., Burns, S.J., Mangini, A., Mudelsee, M., Kramers, J., Villa, I., Neff, U., Al-Subbary, A.A., Buettner, A., Hippler, D., Matter, A., 2007. Holocene ITCZ and Indian monsoon dynamics recorded in stalagmites from Oman and Yemen (Socotra). Quat. Sci. Rev. 26 (1–2), 170–188.

Gasse, F., Fontes, J.C., Campo, E.V., Wei, K., 1996. Holocene environmental changes in Bangong Co basin (Western Tibet). Part 4: discussion and conclusions. Palaeogeogr. Palaeoclimatol. Palaeoecol. 120 (1), 79–92.

Govil, P., Naidu, P.D., 2011. Variations of Indian monsoon precipitation during the last 32 kyr reflected in the surface hydrography of the Western Bay of Bengal. Quat. Sci. Rev. 30 (27–28), 3871–3879.

Gupta, A.K., Anderson, D.M., Overpeck, J.T., 2003. Abrupt changes in the Asian southwest monsoon during the Holocene and their links to the north Atlantic ocean. Nature 421 (6921), 354–357.

He, Y., Hou, J.Z., Brown, E.T., Xie, S.Y., Bao, Z.Y., 2017. Timing of the indian summer monsoon onset during the early Holocene: evidence from a sediment core at linggo Co, central Tibetan plateau. Holocene. https://doi.org/10.1177/0959683617442.

Hillman, A.L., Abbott, M.B., Finkenbinder, M.S., Yu, J.Q., 2017. An 8,600 year lacustrine record of summer monsoon variability from Yunnan, China. Quat. Sci. Rev. 174, 120–132.

Hillman, A.L., Yu, J.Q., Abbott, M.B., Cooke, C.A., Bain, D.J., Steinman, B.A., 2014. Rapid environmental change during dynastic transitions in Yunnan province, China. Quat. Sci. Rev. 98 (15), 24–32.

Hodell, D.A., Brenner, M., Kanfoush, S.L., Curtis, J.H., Stoner, J.S., Song, X.L., Wu, Y., Whitmore, T.J., 1999. Paleoclimate of southwestern China for the past 50000 yr inferred from lake sediment records. Quaternary Research 52 (3), 369–380.

Hofer, S., Tedstone, A.J., Fettweis, X., Bamber, J.L., 2017. Decreasing cloud cover drives the recent mass loss on the Greenland Ice Sheet. Science Advances 3 (6), e1700584.

Hou, J.Z., D'Andrea, W.J., Liu, Z.H., 2012. The influence of ^{14}C reservoir age on interpretation of paleolimnological records from the Tibetan Plateau. Quat. Sci. Rev. 48, 67–79.

Hou, J.Z., D'Andrea, W.J., Wang, M.D., He, Y., Liang, J., 2017. Influence of the Indian

monsoon and the subtropical jet on climate change on the Tibetan Plateau since the late Pleistocene. Quat. Sci. Rev. 163, 84–94.
Jarvis, D.I., 1993. Pollen evidence of changing Holocene monsoon climate in Sichuan Province, China. Quat. Res. 39, 325–337.
Jiang, D.B., Lang, X.M., Tian, Z.P., Wang, T., 2012. Considerable model-data mismatch in temperature over China during the Mid-Holocene: results of PMIP simulations. J. Clim. 25, 4135–4153.
Juggins, S., 2015. Rioja: Analysis of Quaternary Science Data, R Package Version 0.9-9. University of Newcastle, Newcastle upon Tyne.
Juggins, S., Birks, H.J.B., 2012. Quantitative environmental reconstructions from biological data. In: Birks, H.J.B., Lotter, A.F., Juggins, S., Smol, J.P. (Eds.), Tracking Environmental Change Using Lake Sediments: Data Handling and Numerical Techniques. Springer Netherlands, Dordrecht, pp. 431–494.
Kaufman, D.S., Ager, T.A., Anderson, N.J., Anderson, P.M., Andrews, J.T., Bartlein, P.J., Brubaker, L.B., Coats, L.L., Cwynar, L.C., Duvall, M.L., Dyke, A.S., 2004. Holocene thermal maximum in the western Arctic (0-180 W). Quat. Sci. Rev. 23 (5), 529–560.
Kutzbach, J.E., Liu, X.D., Liu, Z.Y., Chen, G.S., 2008. Simulation of the evolutionary response of global summer monsoons to orbital forcing over the past 280,000 years. Clim. Dynam. 30, 567–579.
Leng, M.J., Marshall, J.D., 2004. Palaeoclimate interpretation of stable isotope data from lake sediment archives. Quat. Sci. Rev. 23 (7), 811–831.
Li, J.Y., Xu, Q.H., Zheng, Z., Lu, H.Y., Luo, Y.L., Li, Y.C., Li, C.H., Seppä, H., 2015a. Assessing the importance of climate variables for the spatial distribution of modern pollen data in China. Quat. Res. 83, 287–297.
Li, Y.X., Rao, Z.G., Cao, J.T., Jiang, H., Gao, Y.L., 2016. Highly negative oxygen isotopes in precipitation in southwest China and their significance in paleoclimatic studies. Quat. Int. 440 (part A), 64–71.
Li, Y.X., Rao, Z.G., Liu, X.K., Jin, M., Chen, F.H., 2015b. Interannual correlations between modern precipitation $\delta^{18}O$ and precipitation amount recorded by GNIP stations in China and India. Chin. Sci. Bull. 60, 741–743 (in Chinese).
Liu, J.B., Chen, J.H., Zhang, X.J., Li, Y., Rao, Z.G., Chen, F.H., 2015. Holocene East Asian summer monsoon records in northern China and their inconsistency with Chinese stalagmite $\delta^{18}O$ records. Earth Sci. Rev. 148, 194–208.
Liu, J.B., Chen, S.Q., Chen, J.H., Zhang, Z.P., Chen, F.H., 2017. Chinese cave $\delta^{18}O$ records do not represent northern East Asian summer monsoon rainfall. Proc. Natl. Acad. Sci. Unit. States Am. 114 (15), E2987.
Liu, Y., Li, W.L., He, J.H., Chen, L.X., 2009. Simulation of hydrological cycle changes over China during Mid-Holocene. Acta Meteorol. Sin. 67 (2), 201–209 (in Chinese).
Liu, Y., Zhao, E.X., Huang, W., Zhou, J.Q., Ju, J.H., 2010. Characteristic analysis of precipitation and temperature trend in Yunnan Province in recent 46 years. Journal of Catastrophology 25 (1), 39–37 (in Chinese).
Liu, Y.G., Zhang, M., Liu, Z.Y., Xia, Y., Huang, Y., Peng, Y.R., Zhu, J., 2018. A possible role of dust in resolving the Holocene temperature conundrum. Sci. Rep. 8, 4434. https://doi.org/10.1038/s41598-018-22841-5.
Liu, Z.Y., Zhu, J., Rosenthal, Y., Zhang, X., Otto-Bliesner, B.L., Timmermann, A., Smith, R.S., Lohmann, G., Zheng, W., Timm, O.E., 2014. The Holocene temperature conundrum. Proc. Natl. Acad. Sci. Unit. States Am. 111 (34), E3501–E3505.
Lu, H.Y., Wu, N.Q., Liu, K.B., Zhu, L.P., Yang, X.D., Yao, T.D., Wang, L., Li, Q., Liu, X.Q., Shen, C.M., Li, X.Q., Tong, G.B., Jiang, H., 2011. Modern pollen distributions in Qinghai-Tibetan Plateau and the development of transfer functions for reconstructing Holocene environmental changes. Quat. Sci. Rev. 30, 947–966.
Maher, B.A., 2008. Holocene variability of the East Asian summer monsoon from Chinese cave records: a reassessment. Holocene 18, 861–866.
Marcott, S.A., Shakun, J.D., Clark, P.U., Mix, A.C., 2013. A reconstruction of regional and global temperature for the past 11,300 years. Science 339 (6124), 1198–1201.
Mcmanus, J.F., Francois, R., Gherardi, J.M., Keigwin, L.D., Brown-Leger, S., 2004. Collapse and rapid resumption of Atlantic meridional circulation linked to deglacial climate changes. Nature 428, 834–837.
Menon, S., Hansen, J., Nazarenko, L., Luo, Y., 2002. Climate effects of black carbon aerosols in China and India. Science 297, 2250–2253.
Meyers, P.A., Lallier-Vergès, E., 1999. Lacustrine sedimentary organic matter records of Late Quaternary paleoclimates. J. Paleolimnol. 21 (3), 345–372.
Mishra, P.K., Prasad, S., Anoop, A., Plessen, B., Jehangir, A., Gaye, B., Menzel, P., Weise, S.M., Yousuf, A.R., 2015. Carbonate isotopes from high altitude Tso Moriri Lake (NW Himalayas) provide clues to late glacial and Holocene moisture source and atmospheric circulation changes. Palaeogeogr. Palaeoclimatol. Palaeoecol. 425, 76–83.
Moore, P.D., Webb, J.A., Collinson, M.E., 1991. Pollen Analysis. Blackwell Science, Oxford, pp. 39–62.
Morinaga, H., Itota, C., Isezaki, N., Goto, H., Yaskawa, K., Kusakabe, M., Liu, J., Gu, Z., Cong, S., 1993. Oxygen-18 and carbon-13 records for the last 14,000 years from lacustrine carbonates of Siling-Co (lake) in the Qinghai-Tibetan Plateau. Geophys. Res. Lett. 20 (24), 2909–2912.
Oksanen, J., Blanchet, F.G., Friendly, M., Kindt, R., Legendre, P., McGlinn, D., Minchin, P.R., O'Hara, R.B., Simpson, G.L., Solymos, P., Henry, M., Stevens, H., Szoecs, E., Wagner, H., 2017. Vegan: Community Ecology Package, R Package Version 2.4-2. University of Oulu, Oulu.
Overpeck, J., Anderson, D., Trumbore, S., Prell, W.L., 1996. The southwest Indian Monsoon over the last 18000 years. Clim. Dynam. 12, 213–225.
Pausata, F.S.R., Battisti, D.S., Nisancioglu, K.H., Bitz, C.M., 2011. Chinese stalagmite $\delta^{18}O$ controlled by changes in the Indian monsoon during a simulated Heinrich event. Nat. Geosci. 4, 474–480.
Peterse, F., Martínez-García, A., Zhou, B., Beets, C.J., Prins, M.A., Zheng, H.B., Eglinton, T.I., 2014. Molecular records of continental air temperature and monsoon precipitation variability in East Asia spanning the past 130,000 years. Quat. Sci. Rev. 83 (1), 76–82.
Peterse, F., Prins, M.A., Beets, C.J., Troelstra, S.R., Zheng, H., Gu, Z., Schouten, S., Damsté, J.S.S., 2011. Decoupled warming and monsoon precipitation in East Asia over the last deglaciation. Earth Planet Sci. Lett. 301 (1), 256–264.
R Core Team, 2013. R: a Language and Environment for Statistical Computing. R Foundation for Statistical Computing, Vienna.
Reimer, P.J., Bard, E., Bayliss, A., Beck, J.W., Blackwell, P.G., Ramsey, C.B., Buck, C.E., Cheng, H., Edwards, R.L., Friedrich, M., Grootes, P.M., Guilderson, T.P., Haflidason, H., Hajdas, I., Hatté, C., Heaton, T.J., Hoffmann, D.L., Hogg, A.G., Hughen, K.A., Kaiser, K.F., Kromer, B., Manning, S.W., Niu, M., Reimer, R.W., Richards, D.A., Scott, E.M., Southon, J.R., Staff, R.A., Turney, C.S.M., Plicht, J.v.d, 2013. INTCAL13 and marine 13 radiocarbon age calibration curves 0-50,000 years CAL BP. Radiocarbon 55, 1869–1887.
Renssen, H., Seppä, H., Heiri, O., Roche, D.M., Goosse, H., Fichefet, T., 2009. The spatial and temporal complexity of the Holocene thermal maximum. Nat. Geosci. 2 (6), 411–414.
Roy, S.S., Balling Jr., R.C., 2005. Analysis of trends in maximum and minimum temperature, diurnal temperature range, and cloud cover over India. Geophys. Res. Lett. 32, L12702. https://doi.org/10.1029/2004GL022201.
Schulz, H., von Rad, U., Erlenkeuser, H., 1998. Correlation between Arabian Sea and Greenland climate oscillations of the past 110,000 years. Nature 393, 54–57.
Shen, J., Jones, R.T., Yang, X.D., Dearing, J.A., Wang, S.M., 2006. The Holocene vegetation history of Lake Erhai, Yunnan province southwestern China: the role of climate and human forcing. Holocene 16, 265–276.
Shi, Y.F., Kong, Z.Z., Wang, S.M., Tang, L.Y., Wang, F.B., Yao, T.D., Zhao, X.T., Zhang, P.Y., Shi, S.H., 1993. Mid-Holocene climates and environments in China. Global Planet. Change 7 (1–3), 219–233.
Sinha, A., Kathayat, G., Cheng, H., Breitenbach, S.F., Berkelhammer, M., Mudelsee, M., Biswas, J., Edwards, R.L., 2015. Trends and oscillations in the Indian summer monsoon rainfall over the last two millennia. Nat. Commun. 6 (8), 6309.
Song, X.L., Wu, Y.A., Jiang, Z.W., Long, R.H., Li, B.F., Brenner, M., Whitmore, T.J., Engstrom, D.R., Moore, A., 1994. Paleolimnological Studies on the limestone District in central Yunnan China (In Chinese). Yunnan Science and Technology Press, Kunming.
Sun, X.J., Wu, Y.S., Qiao, Y.L., Walker, D., 1986. Late Pleistocene and Holocene vegetation history at kunming, Yunnan province, southwest China. J. Biogeogr. 13 (5), 441–476.
Tan, M., 2014. Circulation effect: response of precipitation $\delta^{18}O$ to the ENSO cycle in monsoon regions of China. Clim. Dynam. 42, 1067–1077.
Telford, R., Trachsel, M., 2015. PalaeoSig: Significance Tests for Palaeoenvironmental Reconstructions, R packageversion1.1–3. University of Bergen, Bergen.
ter Braak, C.J.F., Juggins, S., 1993. Weighted averaging partial least squares regression (WA-PLS): an improved method for reconstructing environmental variables from species assemblages. Hydrobiologia 269/270, 485–502.
Tian, L.D., Masson-Delmotte, V., Stievenard, M., Yao, T.D., Jouzel, J., 2001. Tibetan Plateau summer monsoon northward extent revealed by measurements of water stable isotopes. Journal of Geophysical Research Atmospheres 106 (D22), 28081–28088.
Tzedakis, P.C., Channell, J.E.T., Hodell, D.A., Kleiven, H.F., Skinner, L.C., 2012. Erratum: determining the natural length of the current interglacial. Nat. Geosci. 5 (2) https://doi.org/10.1038/ngeo1392.
Wang, M., Chen, H., Yu, Z.C., Wu, J.H., Zhu, Q.A., Peng, C.H., Wang, Y.F., Qin, B.Q., 2015. Carbon accumulation and sequestration of lakes in China during the Holocene. Global Change Biol. 21 (12), 4436–4448.
Wang, Y.J., Cheng, H., Edwards, R.L., He, Y.Q., Kong, X.G., An, Z.S., Wu, J.Y., Kelly, M.J., Dykoski, C.A., Li, X.D., 2005. The Holocene Asian monsoon: links to solar changes and North Atlantic climate. Science 308 (5723), 854–857.
Webster, P.J., Magana, V.O., Palmer, T.N., Shukla, J., Tomas, R.A., Yanai, M., Yasunari, T., 1998. Monsoons: processes predictability, and the prospects for prediction. J. Geophys. Res. 103 (C7), 14451–14510.
Wei, K., Gasse, F., 1999. Oxygen isotopes in lacustrine carbonates of west China revisited: implications for post glacial changes in summer monsoon circulation. Quat. Sci. Rev. 18 (12), 1315–1334.
Wei, K.Q., Lin, R.F., 1994. The influence of the monsoon climate on the isotopic composition of precipitation in China. Geochimica 23, 33–41.
Whitmore, T.J., Brenner, M., Song, X.L., 1994. Environmental implications of the late quaternary diatom history from Xingyun hu, Yunnan province, China. Memoir. Calif. Acad. Sci. 17, 525–538.
Wu, D., Zhou, A.F., Chen, X.M., Yu, J.Q., Zhang, J.W., Sun, H.L., 2015b. Hydrological and ecosystem response to abrupt changes in the Indian monsoon during the last glacial, as recorded by sediments from Xingyun Lake, Yunnan, China. Palaeogeogr. Palaeoclimatol. Palaeoecol. 421, 15–23.
Wu, D., Zhou, A.F., Liu, J.B., Chen, X.M., Wei, H.T., Sun, H.L., Yu, J.Q., Bloemendal, J., Chen, F.H., 2015a. Changing intensity of human activity over the last 2,000 years recorded by the magnetic characteristics of sediments from Xingyun Lake, Yunnan, China. J. Paleolimnol. 53, 47–60.
Xiao, X.Y., Haberle, S.G., Shen, J., Yang, X.D., Han, Y., Zhang, E.L., Wang, S.M., 2014. Latest Pleistocene and Holocene vegetation and climate history inferred from an alpine lacustrine record, northwestern Yunnan province, southwestern China. Quat. Sci. Rev. 86 (86), 35–48.
Xie, S.C., Evershed, R.P., Huang, X.Y., Zhu, Z.M., Pancost, R.D., Meyers, P.A., Gong, L.F., Hu, C.Y., Huang, J.H., Zhang, S.H., Gu, Y.S., Zhu, J.Y., 2013. Concordant monsoon-

driven postglacial hydrological changes in peat and stalagmite records and their impacts on prehistoric cultures in central China. Geology 41, 827–830.
Xu, Q.H., Xiao, J.L., Li, Y.C., Tian, F., Nakagawa, T., 2010. Pollen-based quantitative reconstruction of Holocene climate changes in the daihai lake area, inner Mongolia, China. J. Clim. 2856–2868.
Yao, T.D., Thompson, L., Yang, W., Yu, W.S., Gao, Y., Guo, X.J., Yang, X.X., Duan, K.Q., Zhao, H.B., Xu, B.Q., Pu, J.C., Xiang, Y., Kattel, D., Joswiak, D., 2012. Different glacier status with atmospheric circulations in Tibetan Plateau and surroundings. Nat. Clim. Change 2 (9), 663–667.
Yu, S.C., Li, P.F., Wang, L.Q., Wang, P., Wang, S., Chang, S.C., Liu, W.P., Alapaty, K., 2016. Anthropogenic aerosols are a potential cause for migration of the summer monsoon rain belt in China. Proc. Natl. Acad. Sci. Unit. States Am. 113, E2209–E2210.
Yu, W.S., Yao, T.D., Tian, L.D., Ma, Y.M., Ichiyanagi, K., Wang, Y., Sun, W.Z., 2008. Relationships between $\delta^{18}O$ in precipitation and air temperature and moisture origin on a south-north transect of the Tibetan Plateau. Atmos. Res. 87 (2), 158–169.
Zhang, E.L., Chang, J., Cao, Y.M., Sun, W.W., Shulmeister, J., Tang, H.Q., Langdon, P.G., Yang, X.D., Shen, J., 2017a. Holocene high-resolution quantitative summer temperature reconstruction based on subfossil chironomids from the southeast margin of the Qinghai-Tibetan plateau. Quat. Sci. Rev. 165, 1–12.
Zhang, H.L., Li, S.J., Feng, Q.L., Zhang, S.T., 2010. Environmental change and human activities during the 20th century reconstructed from the sediment of Xingyun Lake, Yunnan Province, China. Quat. Int. 212 (1), 14–20.
Zhang, J.W., Chen, F.H., Holmes, J.A., Li, H., Guo, X.Y., Wang, J.L., Li, S., Lü, Y.B., Zhao, Y., Qiang, M.R., 2011a. Holocene monsoon climate documented by oxygen and carbon isotopes from lake sediments and peat bogs in China: a review and synthesis. Quat. Sci. Rev. 30, 1973–1987.
Zhang, Q., Li, Y.Q., Chen, Q.L., Ren, J.X., 2011b. Temporal and spatial distributions of cloud cover over southwest China in recent 46 years. Plateau Meteorol. 30 (2), 339–348 (in Chinese).
Zhang, S.T., Song, X.L., Zhang, Z.X., Feng, Q.L., Liu, B.P., 2003. The changing of mineral composition and environmental significance in surface sediments of Xingyun Lake. Adv. Earth Sci. 18 (6), 928–932 (in Chinese).
Zhang, W.X., Ming, Q.Z., Shi, Z.T., Chen, G.J., Niu, J., Lei, G.L., Chang, F.Q., Zhang, H.C., 2014. Lake sediment records on climate change and human activities in the Xingyun lake catchment, SW China. PLoS One 9 (7), e102167.
Zhang, Y., Renssen, H., Seppä, H., Valdes, P.J., 2017b. Holocene temperature evolution in the Northern Hemisphere high latitudes-Model-data comparisons. Quat. Sci. Rev. 173, 101–113.
Zhao, Y.S., Zhao, X.F., 1988. Modern lake basin sedimentation at Jiangchuan, Yunnan. J. Chengdu Univ. Technol. (Sci. Technol. Ed.) 15 (3), 83–92 (in Chinese).
Zheng, Z., Wei, J., Huang, K., Xu, Q.H., Lu, H., Tarasov, P., Luo, C., Beaudouin, C., Deng, Y., Pan, A., Zheng, Y., Luo, Y., Nakagawa, T., Li, C., Yang, S., Peng, H., Cheddadi, R., 2014. East Asian pollen database: modern pollen distribution and its quantitative relationship with vegetation and climate. J. Biogeogr. 41, 1819–1832.
Zhou, A.F., He, Y.X., Wu, D., Zhang, X.N., Zhang, C., Liu, Z.H., Yu, J.Q., 2015. Changes in the radiocarbon reservoir age in Lake Xingyun, southwestern China during the Holocene. PLoS One. https://doi.org/10.1371/journal.pone.0121532.
Ziegler, M., Tuenter, E., Lourens, L.J., 2010. The precession phase of the boreal summer monsoon as viewed from the eastern Mediterranean (ODP Site 968). Quat. Sci. Rev. 29, 1481–1490.
Zielinski, G.A., Mershon, G.R., 1997. Paleoenvironmental implications of the insoluble microparticle record in the GISP2 (Greenland) ice core during the rapidly changing climate of the Pleistocene-Holocene transition. Geol. Soc. Am. Bull. 109, 547–559.